The American Journal of Human Genetics, Volume *106*

Supplemental Data

Mutations in the Kinesin-2 Motor *KIF3B* Cause an Autosomal-Dominant Ciliopathy

Benjamin Cogné, Xenia Latypova, Lokuliyanage Dona Samudita Senaratne, Ludovic Martin, Daniel C. Koboldt, Georgios Kellaris, Lorraine Fievet, Guylène Le Meur, Dominique Caldari, Dominique Debray, Mathilde Nizon, Eirik Frengen, Sara J. Bowne, 99 Lives Consortium, Elizabeth L. Cadena, Stephen P. Daiger, Kinga M. Bujakowska, Eric A. Pierce, Michael Gorin, Nicholas Katsanis, Stéphane Bézieau, Simon M. Petersen-Jones, Laurence M. Occelli, Leslie A. Lyons, Laurence Legeai-Mallet, Lori S. Sullivan, Erica E. Davis, and Bertrand Isidor

SUPPLEMENTARY INFORMATION

Supplementary Note. Recessive mutations in *KIF3B* cause retinal degeneration in Bengal cats.

As part of our ongoing work to identify the molecular underpinnings of clinically relevant traits in the domestic cat (*Felis silvestris catus*), we previously reported a recessively segregating progressive retinal atrophy (PRA) in the Bengal cat[1]. Mutant kittens show an early reduction in rod function and an early and progressive loss of outer retinal structure[1].

To determine the genetic change(s) responsible for this condition, we performed a genome-wide association study (GWAS) on 98 Bengal cats (44 cases and 54 controls) on the 63K feline SNP array (University of Missouri IACUC protocol 8313; Supplementary Methods). Bengal cats were originally donated, with written consent, by Bengal breeders for the establishment of a breeding colony. Cases and controls were either from Bengal cat owners or selected from the research colony[1]. All cases were confirmed by a board-certified veterinary ophthalmologist at the University of California-Davis Veterinary Medical Teaching Hospital or the MU Veterinary Health Center Ophthalmological Services. The genotyping rate was 0.99. Overall, 147 SNPs failed the missingness test (GENO > 0.2), 15,986 SNPs failed the frequency test (MAF < 0.05), leaving 46,821 SNPs for the GWAS. The GWAS indicated several SNPs in high association with the blindness phenotype on cat chromosome A3 (Table S5, Figure 3A). Several SNPs were significant in several regions of cat chromosome A3, suggesting assembly errors.

To delineate further the genetic cause of progressive retinal atrophy in these Bengal cats, we performed whole genome sequencing, as part of the 99 Lives Cat Genome Sequencing Initiative (Accession: PRJNA308208; BioProject PRJNA343385; Supplementary Methods),3/27/20 10:53:00 AM on a trio of cats from the research colony. The trio included an obligate carrier sire (S13227), a blind queen (S15240) and a female blind offspring (S17799). Seven additional obligate carriers were in the 99 Lives dataset as well as one Bengal cat of unknown status (S20423). An average of ~30X sequencing coverage per cat was achieved.[3] Genome alignment was to cat genome assembly GCF_000181335.3 FELIS_CATUS_9.0, annotation was Ensembl release 94 and variant calling was performed as described[6] and variants were filtered using VarSeq software from Golden Helix (Bozeman, MT). We prioritized variants by their effect on the protein using SnpEff.[7] The GWAS had localized the progressive retinal atrophy locus to cat chromosome A3 (Figure 3A), therefore, we scanned the entire A3 cat chromosome for disease-causing genes and considered all variants that had expected inheritance in the trio, (i.e. homozygous in the two affected cats and heterozygous in the obligate carriers (n = 8; Figure 3A, Table S6). The Bengal cat in the dataset of unknown disease status was excluded from the analysis. We identified only two homozygous variants in the two affected cats, which reside in the genes *CHD6* and *KIF3B*, respectively. All obligate carriers were heterozygous for the *KIF3B* variant. The purebred Bengal

cat of unknown status was also heterozygous for the *KIF3B* variant, indicating that this cat was a carrier. The nonsynonymous *KIF3B* change, ENSFCAT00000022266:c.1000G>A, causes a p.Ala334Thr amino acid change, is positioned within the kinesin motor domain (Figure S5), and is predicted to be pathogenic by SIFT[8] and PolyPhen-2[9].

We performed phenotyping at Michigan State University in accordance with an approved institutional animal care and use committee protocol (IACUC; Figure 3B; Supplementary Methods). We reported previously that the first ophthalmoscopic signs of retinal degeneration in affected cats appear at 8 weeks of age, with visual deficits behaviorally evident by 1 year of age. Concordantly, by 8-weeks of age, we observed thinning of the outer retinal layers including the outer nuclear layer (ONL) and loss of definition of the layers representing photoreceptor inner and outer segments (Figure 3B). Immunodetection of Kif3b in the wild-type (WT) animal labelled the inner segment and the inner segment/outer segment junction (Figure 3B; Table S3). In retinal sections from an 8-week-old *KIF3B* mutant, Kif3b was detectable with antibody staining at the inner segments with some mislocalization to the outer portion of the ONL and a blurred demarcation between inner segment and outer segment by comparison to the WT control. However, by 20 weeks of age when the ONL was markedly thinned, Kif3b labeling was barely detectable in mutant felines (Figure 3B). To investigate possible correlates between Kif3b mutation and localization of phototransduction cascade components, we labelled cone markers, ML opsin (MLO) and peanut agglutin (PNA), and a rod marker, rhodopsin Ab-1 (RetP1), respectively (Table S3). At 8 weeks of age, mutant kittens displayed normal cone morphology while there was modest rhodopsin mislocalization to inner segments. By 20 weeks of age, we noted stunting of cone inner and outer segments and marked rod opsin mislocalization to the ONL. At 34 weeks of age, only one or two rows of photoreceptor nuclei remained and we observed loss of cone inner and outer segments with only some material external to the outer limiting membrane still immunopositive for the cone markers; rod opsin mislocalization was still prominent.

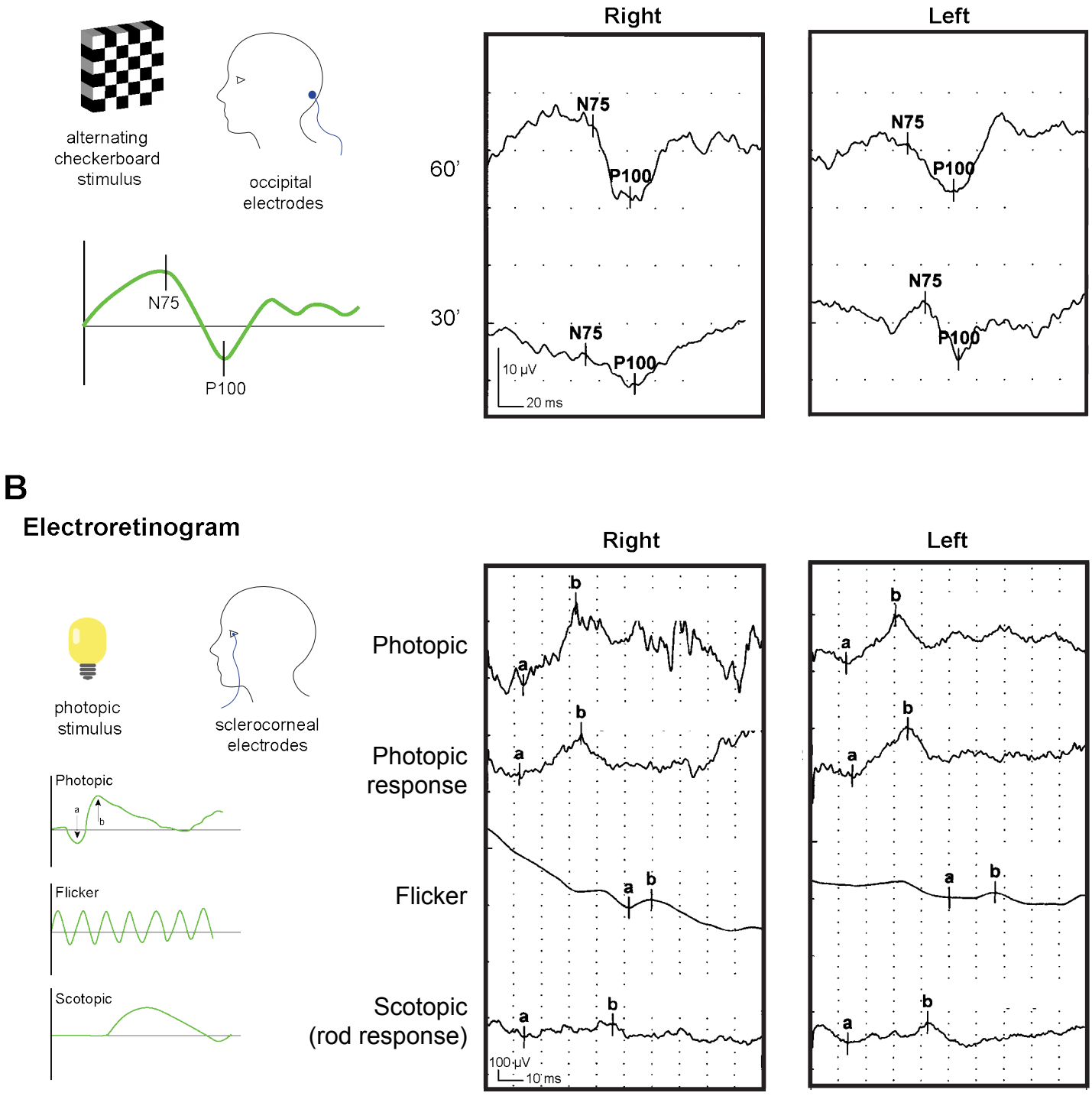
A
Visual evoked potential
alternating checkerboard stimulus
occipital electrodes
N75
P100
Right
Left
60'
30'
N75
P100
10 µV
20 ms
B
Electroretinogram
photopic stimulus
sclerocorneal electrodes
Photopic
Flicker
Scotopic
Photopic response
Flicker
Scotopic (rod response)
a
b
100 µV
10 ms

Figure S1

Figure S1. Functional vision evaluation of Individual 1.

(A) Left, recording system and expected result for evoked visual potential. Right, electroretinogram (ERG) of individual 1 (family A) showing an alteration of peripheral retinal responses.

(B) Electroretinogram. Left, recording system and expected result for evoked visual potential. Right, photopic, photopic response, flicker and scotopic response of individual 1. ERG recordings were acquired according to the International Society for Clinical Electrophysiology of Vision (ISCEV) protocol and were performed on a vision monitor (Monpack3, Metrovision, Perenchies, France).

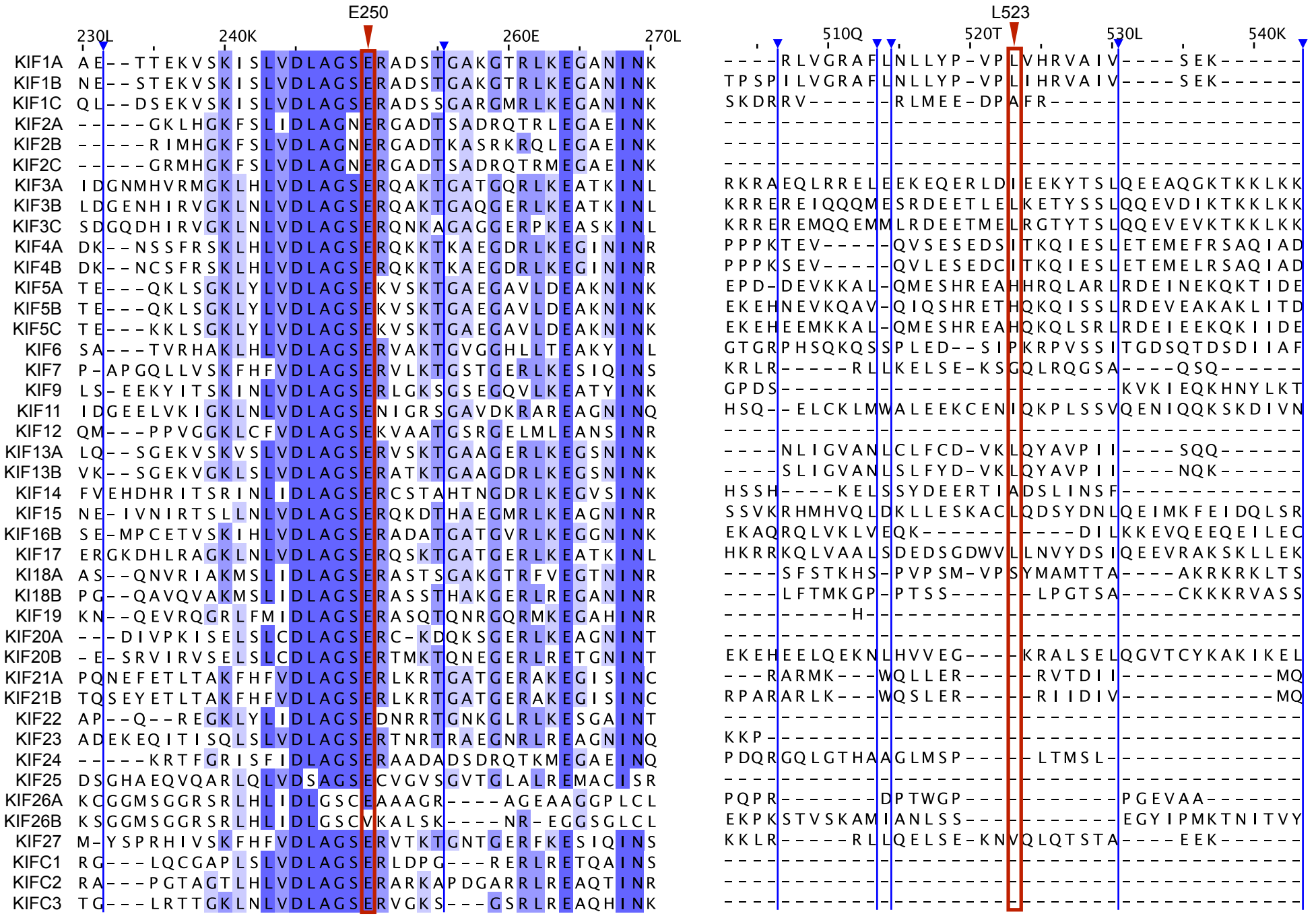
E250
230L
240K
260E
270L
KIF1A AE--TTEKVSKISLVDLAGSERADSTGAKGTRLKEGANINK
KIF1B NE--STEKVSKISLVDLAGSERADSTGAKGTRLKEGANINK
KIF1C QL--DSEKVSKISLVDLAGSERADSSGARGMRLKEGANINK
KIF2A ------GKLHGKFSLIDLAGNERGADTSADRQTRLEGAEINK
KIF2B ------RIMHGKFSLVDLAGNERGADTKASRKRQLEGAEINK
KIF2C ------GRMHGKFSLVDLAGNERGADTSADRQTRMEGAEINK
KIF3A IDGNMHVRMGKLHLVDLAGSERQAKTGATGQRLKEATKINL
KIF3B LDGENHIRVGKLNLVDLAGSERQAKTGAQGERLKEATKINL
KIF3C SDGQDHIRVGKLNLVDLAGSERQNKAGAGGERPKEASKINL
KIF4A DK--NSSFRSKLHLVDLAGSERQKKTKAEGDRLKEGININR
KIF4B DK--NCSFRSKLHLVDLAGSERQKKTKAEGDRLKEGININR
KIF5A TE---QKLSGKLYLVDLAGSEKVSKTGAEGAVLDEAKNINK
KIF5B TE---QKLSGKLYLVDLAGSEKVSKTGAEGAVLDEAKNINK
KIF5C TE---KKLSGKLYLVDLAGSEKVSKTGAEGAVLDEAKNINK
KIF6 SA---TVRHAKLHLVDLAGSERVAKTGVGGHLLTEAKYINL
KIF7 P-APGQLLVSKFHFVDLAGSERVLKTGSTGERLKESIQINS
KIF9 LS-EEKYITSKINLVDLAGSERLGKSGSEGQVLKEATYINK
KIF11 IDGEELVKIGKLNLVDLAGSENIGRSGAVDKRAREAGNINQ
KIF12 QM---PPVGGKLCFVDLAGSEKVAATGSRGELMLEANSINR
KIF13A LQ--SGEKVSKVSLVDLAGSERVSKTGAAGERLKEGSNINK
KIF13B VK--SGEKVGKLSLVDLAGSERATKTGAAGDRLKEGSNINK
KIF14 FVEHDHRITSRINLIDLAGSERCSTAHTNGDRLKEGVSINK
KIF15 NE-IVNIRTSLLNLVDLAGSERQKDTHAEGMRLKEAGNINR
KIF16B SE-MPCETVSKIHLVDLAGSERADATGATGVRLKEGGNINK
KIF17 ERGKDHLRAGKLNLVDLAGSERQSKTGATGERLKEATKINL
KI18A AS--QNVRIAKMSLIDLAGSERASTSGAKGTRFVEGTNINR
KI18B PG--QAVQVAKMSLIDLAGSERASSTHAKGERLREGANINR
KIF19 KN--QEVRQGRLFMIDLAGSERASQTQNRGQRMKEGAHINR
KIF20A ---DIVPKISELSLCDLAGSERC-KDQKSGERLKEAGNINT
KIF20B -E-SRVIRVSELSLCDLAGSERTMKTQNEGERLRETGNINT
KIF21A PQNEFETLTAKFHFVDLAGSERLKRTGATGERAKEGISINC
KIF21B TQSEYETLTAKFHFVDLAGSERLKRTGATGERAKEGISINC
KIF22 AP--Q--REGKLYLIDLAGSEDNRRTGNKGLRLKESGAINT
KIF23 ADEKEQITISQLSLVDLAGSERTNRTRAEGNRLREAGNINQ
KIF24 -----KRTFGRISFIDLAGSERAADADSDRQTKMEGAEINQ
KIF25 DSGHAEQVQARLQLVDSAGSECVGVSGVTGLALREMACISR
KIF26A KCGGMSGGRSRLHLIDLGSCEAAAGR----AGEAAGGPLCL
KIF26B KSGGMSGGRSRLHLIDLGSCVKALSK----NR-EGGSGLCL
KIF27 M-YSPRHIVSKFHFVDLAGSERVTKTGNTGERFKESIQINS
KIFC1 RG---LQCGAPLSLVDLAGSERLDPG---RERLRETQAINS
KIFC2 RA---PGTAGTLHLVDLAGSERARKAPDGARRLREAQTINR
KIFC3 TG---LRTTGKLNLVDLAGSERVGKS---GSRLREAQHINK
L523
510Q
520T
530L
540K
----RLVGRAFLNLLYP-VPLVHRVAIV----SEK------
TPSPILVGRAFLNLLYP-VPLIHRVAIV----SEK------
SKDRRV-----RLMEE-DPAFR----------------
RKRAEQLRRELEEKEQERLDIEEKYTSLQEEAQGKTKKLKK
KRREREIQQQMESRDEETLELKETYSSLQQEVDIKTKKLKK
KRREREMQQEMMLRDEETMELRGTYTSLQQEVEVKTKKLKK
PPPKTEV-----QVSESEDSITKQIESLETEMEFRSAQIAD
PPPKSEV-----QVLESEDCITKQIESLETEMELRSAQIAD
EPD-DEVKKAL-QMESHREAHHRQLARLRDEINEKQKTIDE
EKEHNEVKQAV-QIQSHRETHQKQISSLRDEVEAKAKLITD
EKEHEEMKKAL-QMESHREAHQKQLSRLRDEIEEKQKIIDE
GTGRPHSQKQSSPLED--SIPKRPVSSITGDSQTDSDIIAF
KRLR-----RLLKELSE-KSGQLRQGSA----QSQ------
GPDS-----------------------KVKIEQKHNYLKT
HSQ--ELCKLMWALEEKCENIQKPLSSVQENIQQKSKDIVN
----NLIGVANLCLFCD-VKLQYAVPII----SQQ------
----SLIGVANLSLFYD-VKLQYAVPII----NQK------
HSSH----KELSSYDEERTIADSLINSF----------
SSVKRHMHVQLDKLLESKACLQDSYDNLQEIMKFEIDQLSR
EKAQRQLVKLVEQK----------DILKKEVQEEQEILEC
HKRRKQLVAALSDEDSGDWVLLNVYDSIQEEVRAKSKLLEK
----SFSTKHS-PVPSM-VPSYMAMTTA----AKRKRKLTS
----LFTMKGP-PTSS-----LPGTSA----CKKKRVASS
----------H----------
EKEHEELQEKNLHVVEG----KRALSELQGVTCYKAKIKEL
---RARMK---WQLLER-----RVTDII----------MQ
RPARARLK---WQSLER-----RIIDIV----------MQ
KKP----------
PDQRGQLGTHAAGLMSP-----LTMSL----------
PQPR-------DPTWGP----------PGEVAA------
EKPKSTVSKAMIANLSS----------EGYIPMKTNITVY
KKLR-----RLLQELSE-KNVQLQTSTA----EEK------

Figure S2

Figure S2. Molecular motor domain residue Glu250 is highly conserved across human kinesins. Multiple-sequence alignment (Clustal O v1.2.4) of 42 human kinesin proteins sorted by pair-wise identity. Color indicates percent identity. Blue arrow head, insertions; red arrow, Glu250 (left) or Leu523 (right) residues. KIF1A: Q12756, KIF1B: O60333, KIF1C: O43896, KIF2A: O00139, KIF2B: Q8N4N8, KIF2C: Q99661, KIF3A: Q9Y496, KIF3B: O15066, KIF3C: O14782, KIF4A: O95239, KIF4B: Q2VIQ3, KIF5A: Q12840, KINH: P33176, KIF5C: O60282, KIF6: Q6ZMV9, KIF7: Q2M1P5, KIF9: Q9HAQ2, KIF11: P52732, KIF12: Q96FN5, KI13A: Q9H1H9, KI13B: Q9NQT8, KIF14: Q15058, KIF15: Q9NS87, KI16B: Q96L93, KIF17: Q9P2E2, KI18A: Q8NI77, KI18B: Q86Y91, KIF19: Q2TAC6, KI20A: O95235, KI20B: Q96Q89, KI21A: Q7Z4S6, KI21B: O75037, KIF22: Q14807, KIF23: Q02241, KIF24: Q5T7B8, KIF25: Q9UIL4, KI26A: Q9ULI4, KI26B: Q2KJY2, KIF27: Q86VH2, KIFC1: Q9BW19, KIFC2: Q96AC6, KIFC3: Q9BVG8.

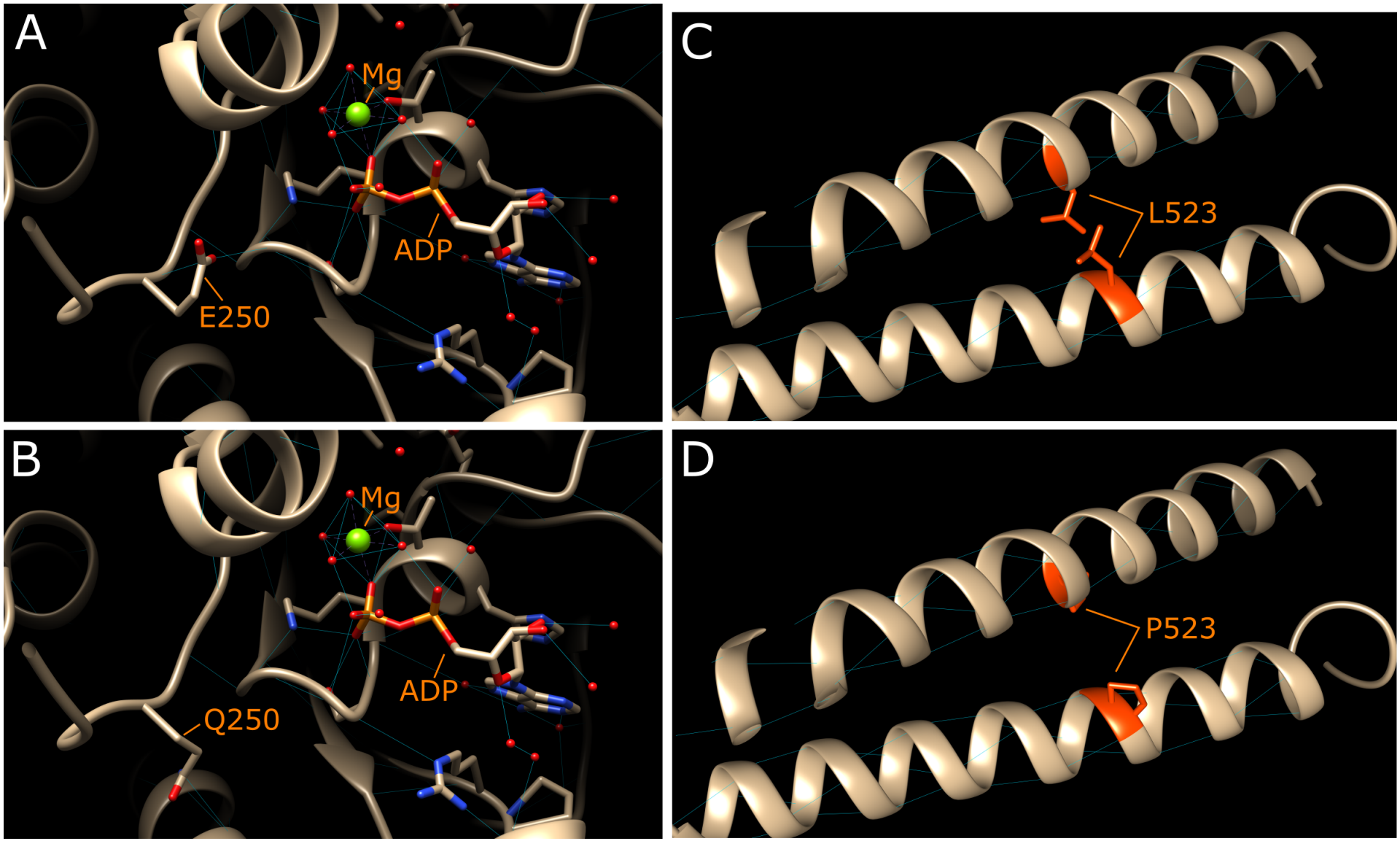

Figure S3

Figure S3. Mutated human KIF3B residues represented on a 3D structure.

(A) The crystallography of the human ubiquitous kinesin motor domain (PDB:1BG2) with magnesium (Mg) and ADP was used to visualize p.Glu250 amino acid. Hydrogen bonds are shown with blue bars. (B) p.Glu250 residue replaced by a Glutamine.

(C) Structure of the KIF3B coiled coil domain was built with SWISS-MODEL as no crystal structure was available for p.Leu523. The corresponding Leucine is depicted.

(D) p.Leu523 residue replaced by a Proline. UCSF chimera software was used for modelling.

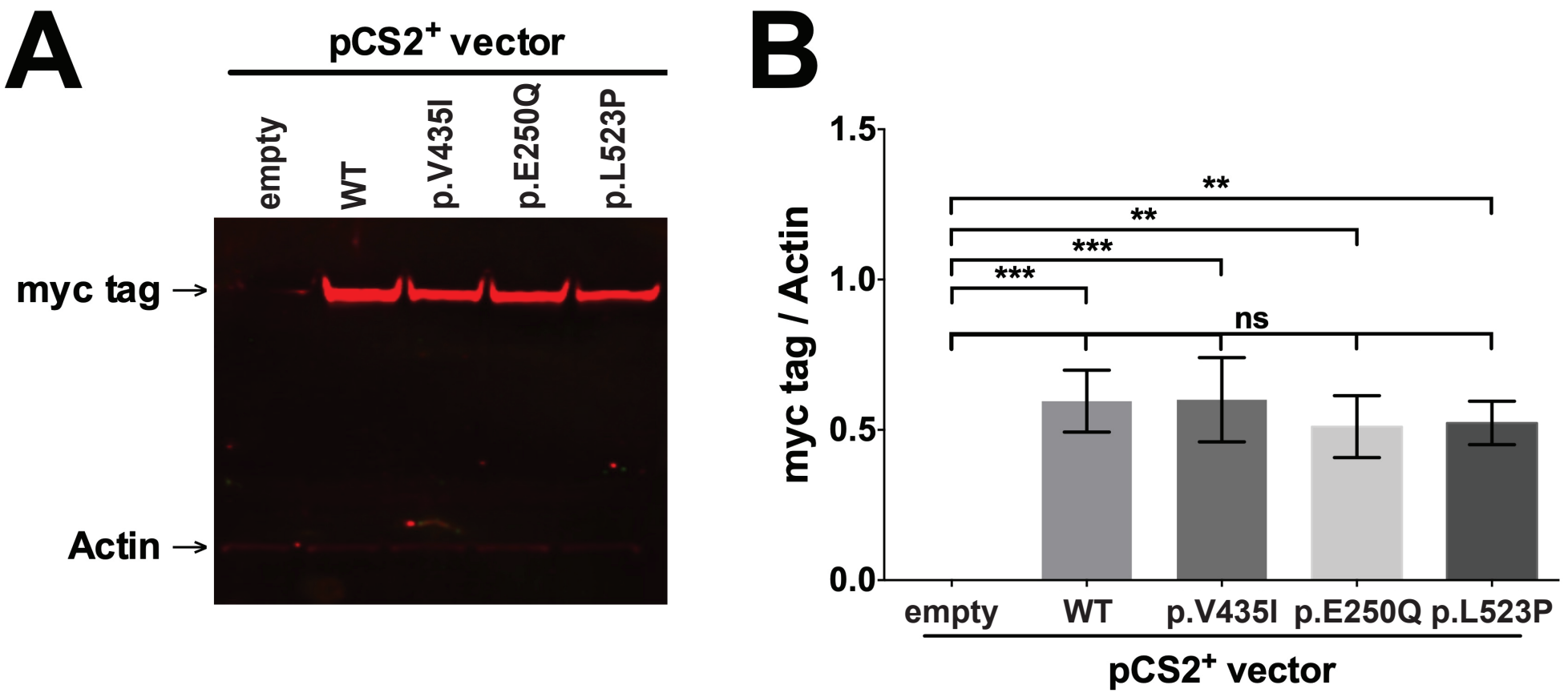
A
pCS2+ vector
empty
WT
p.V435I
p.E250Q
p.L523P
myc tag →
Actin →
B
myc tag / Actin
1.5
1.0
0.5
0.0
**
**
***
***
ns
empty
WT
p.V435I
p.E250Q
p.L523P
pCS2+ vector

Figure S4

Figure S4. Transient expression of KIF3B-myc in HEK293 cells.

(A) Western blot analysis of myc tag (KIF3B expression) and actin in HEK293 cells transiently transfected with pCS2^{+}-empty, pCS2^{+}-*KIF3B-WT-myc*, pCS2^{+}-*KIF3B-V435I-myc*, pCS2^{+}-*KIF3B-E250Q-myc*, pCS2^{+}-*KIF3B-L523P-myc* vectors (48h post transfection).

(B) Quantitative analysis of myc tag (KIF3B expression) normalized to actin in HEK293 cells transiently transfected with pCS2^{+}-empty, pCS2^{+}-*KIF3B-WT-myc*, pCS2^{+}-*KIF3B-V435I-myc*, pCS2^{+}-*KIF3B-E250Q-myc*, pCS2^{+}-*KIF3B-L523P-myc* vectors (48h post transfection). Performed on six independent experiments. Error bars indicate standard error of the mean (s.e.m.).

A

KIF3B (*Felis catus*)
M3X169

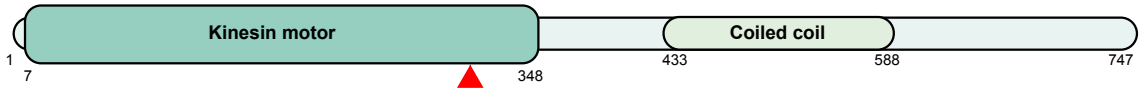

B

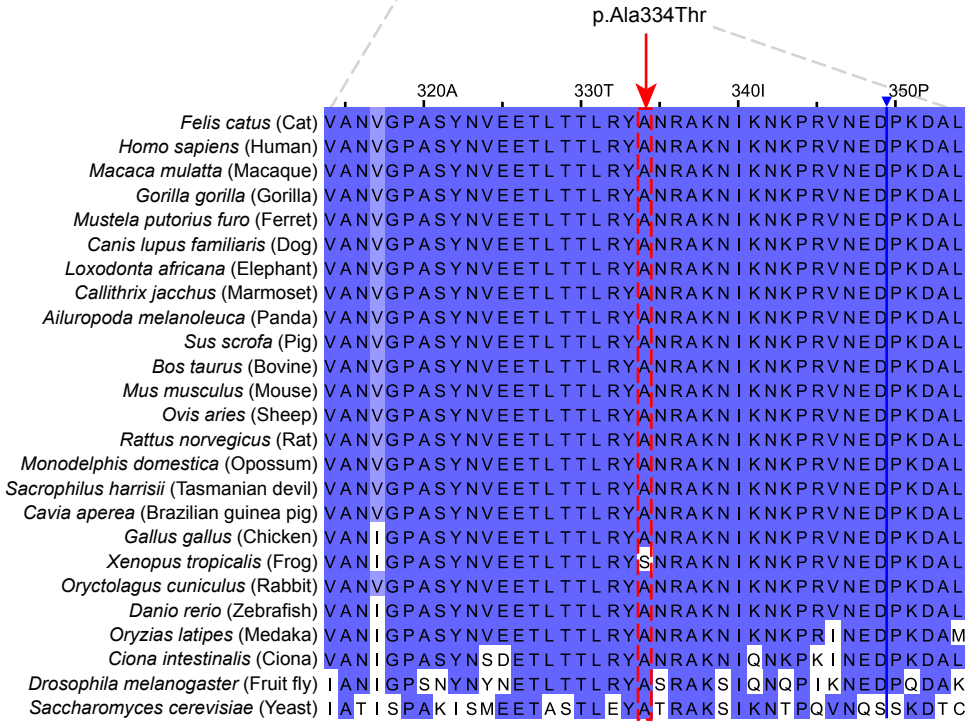

C

KIF3B (*Felis catus*)
M3X169

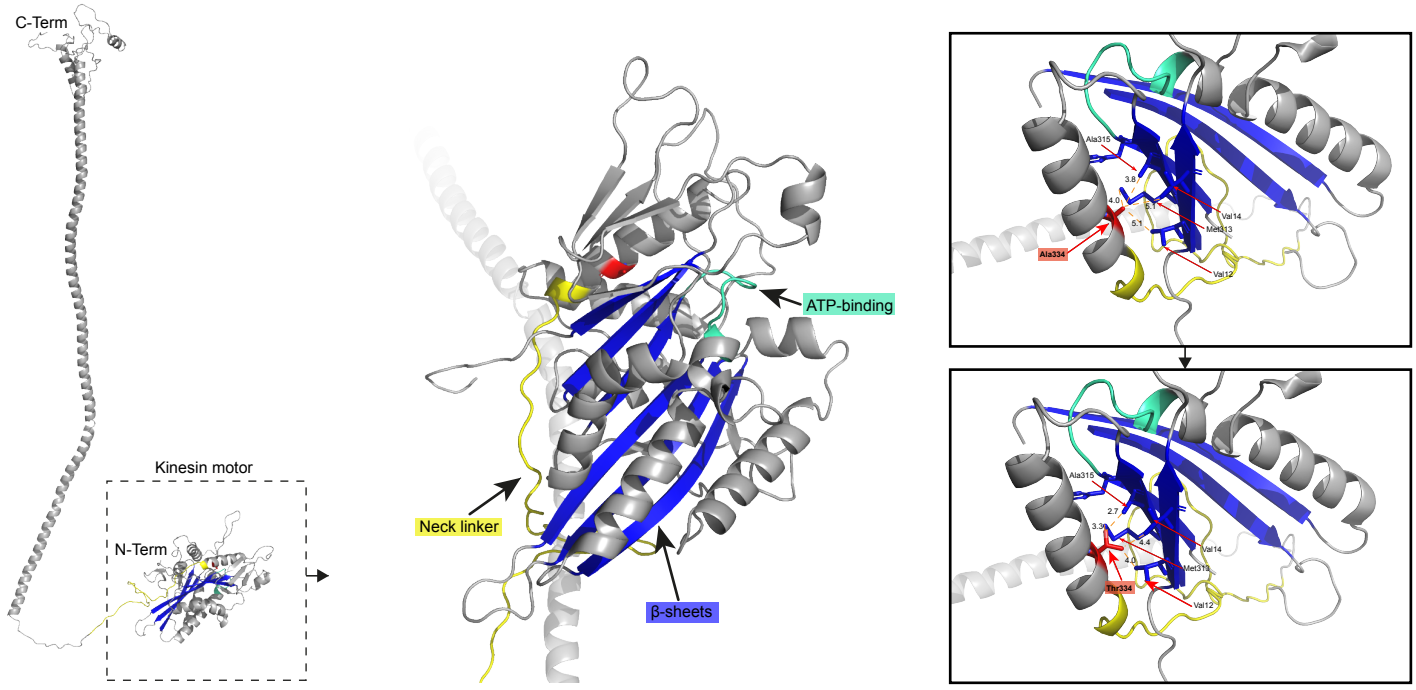

Figure S5

Figure S5. Protein structure and amino acid conservation of domestic cat KIF3B p.Ala334Thr.

(A) Schematic of *Felis catus* (cat) KIF3B protein structure. Red arrow head, *KIF3B* c.1000G>A, Ala334Thr variant; Kinesin motor and coiled coil domains (UniProtKB identifier M3X169, PROSITE annotations) are indicated.

(B) *Felis catus* KIF3B protein sequence block impacted by the p.Ala334Thr nonsynonymous change and multiple sequence alignment of 40 amino acid blocks of cat, human and 23 additional species sorted by pairwise identity compared to the human KIF3B protein sequence (Clustal W v1.81). Red box, variant residue; blue shading of amino acids from dark to light represents most to least conserved, respectively. UniProtKB identifiers: *Homo sapiens*, O15066; *Macaca mulatta*, F6S877; *Gorilla gorilla*, G3RAF7; *Mustela putorius furo*, M3Z2F0; *Canis lupus familiaris*, E2QUS2; *Loxodonta africana*, G3T0G8; *Callithrix jacchus*, F7IBN6; *Ailuropoda melanoleuca*, G1M429; *Felis catus*, A0A2I2UKW2; *Sus scrofa*, F1S519; *Bos taurus*, F1N020; *Mus musculus*, Q61771; *Ovis aries*, W5NZV7; *Rattus norvegicus*, D3ZI07; *Monodelphis domestica*, F6RWN1; *Sarcophilus harrisii*, G3WA27; *Cavia aperea*, ENSCAPP00000010080 (ensembl, UniProtKB identifier not available); *Gallus gallus*, Q5F423; *Xenopus tropicalis*, F6R640; *Oryctolagus cuniculus*, G1U1D0; *Danio rerio*, F1QN54; *Oryzias latipes*, H2LAE9; *Ciona intestinalis*, F7B875; *Drosophila melanogaster*, P46867; *Saccharomyces cerevisiae*, P28742.

(C) *In silico* protein modeling of *Felis catus* KIF3B nonsynonymous variant. Left, three dimensional *in silico* view of *Felis catus* KIF3B protein structure (UniProtKB identifier M3X169). Middle, kinesin motor domain impacted by p.Ala334Thr change is shown. Neck linker, ATP-binding and ß-sheets are indicated in yellow, green and blue, respectively. Right, distance (Å) between side chains of wild type (Ala334; upper box) and mutant (Thr334; lower box) KIF3B and the closest residue on the opposing side of the protein are measured as indicated (orange dashed lines). Protein Data Bank (PDB) file was generated by RaptorX and analyzed in Pymol 2.0.

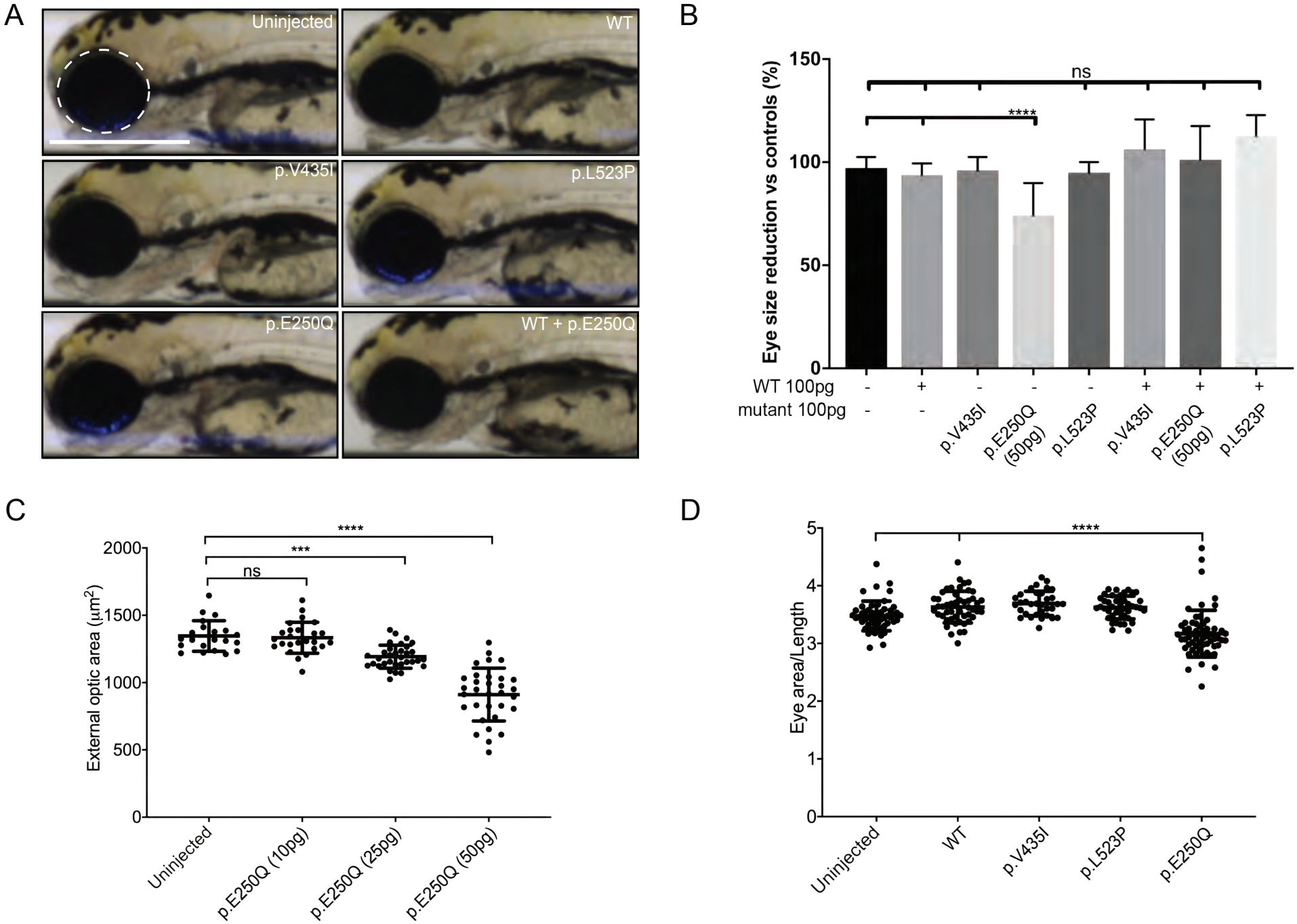
A
Uninjected
WT
p.V435I
p.L523P
p.E250Q
WT + p.E250Q
B
Eye size reduction vs controls (%)
150
100
50
0
ns
****
WT 100pg - + - - - + + +
mutant 100pg - - p.V435I p.E250Q (50pg) p.L523P p.V435I p.E250Q (50pg) p.L523P
C
External optic area (µm²)
2000
1500
1000
500
0
****
***
ns
Uninjected
p.E250Q (10pg)
p.E250Q (25pg)
p.E250Q (50pg)
D
Eye area/Length
5
4
3
2
1
0
****
Uninjected
WT
p.V435I
p.L523P
p.E250Q

Figure S6

Figure S6. Eye size in zebrafish larvae with heterologous mutant *KIF3B* expression and normalization of eye size phenotype to zebrafish larval body length.

(A) Representative bright field lateral images of 3-day post fertilization (dpf) larvae captured with the onboard camera attached to the VAST Bioimager system (Union Biometrica). Scale bar: 550 μm, with equivalent scaling for each condition.

(B) Quantification of larval eye area at 3 dpf in the context of human *KIF3B* mRNA (dashed white circle in panel (A). We observed a 20% reduction in mean eye size for p.Glu250Gln mRNA vs WT or uninjected controls. n=50-60 larvae per condition, repeated. Error bars indicate standard deviation (s.d.).

(C) Quantification of external optic area in larval batches injected with a *KIF3B* p.Glu250Gln mRNA dosage curve to determine an optimal dose for phenotyping that does not induce significant lethality at 3 days post fertilization (dpf). See Figure 5A for representative images and region measured. n=60-70 larvae/condition, repeated twice with similar results. Error bars indicate standard deviation (s.d.).

(B) Plot of eye area (μm^2) to body length (μm) ratio to confirm that optic size reduction is not due to developmental delay in *KIF3B* mRNA-injected larvae at 3 dpf.

Non-parametric one-way ANOVA followed by Tukey's multiple comparison (GraphPad PRISM software; version 7.0c). **** $p<0.0001$. ns, not significant; WT, wild type; p.Glu250Gln and p.Leu523Pro are variants identified in cases; p.Val435Ile is a negative control (rs41288638; 230/276,748 alleles in gnomAD). n=40-50 larvae/condition, repeated twice with similar results. Error bars indicate standard deviation (s.d.).

A

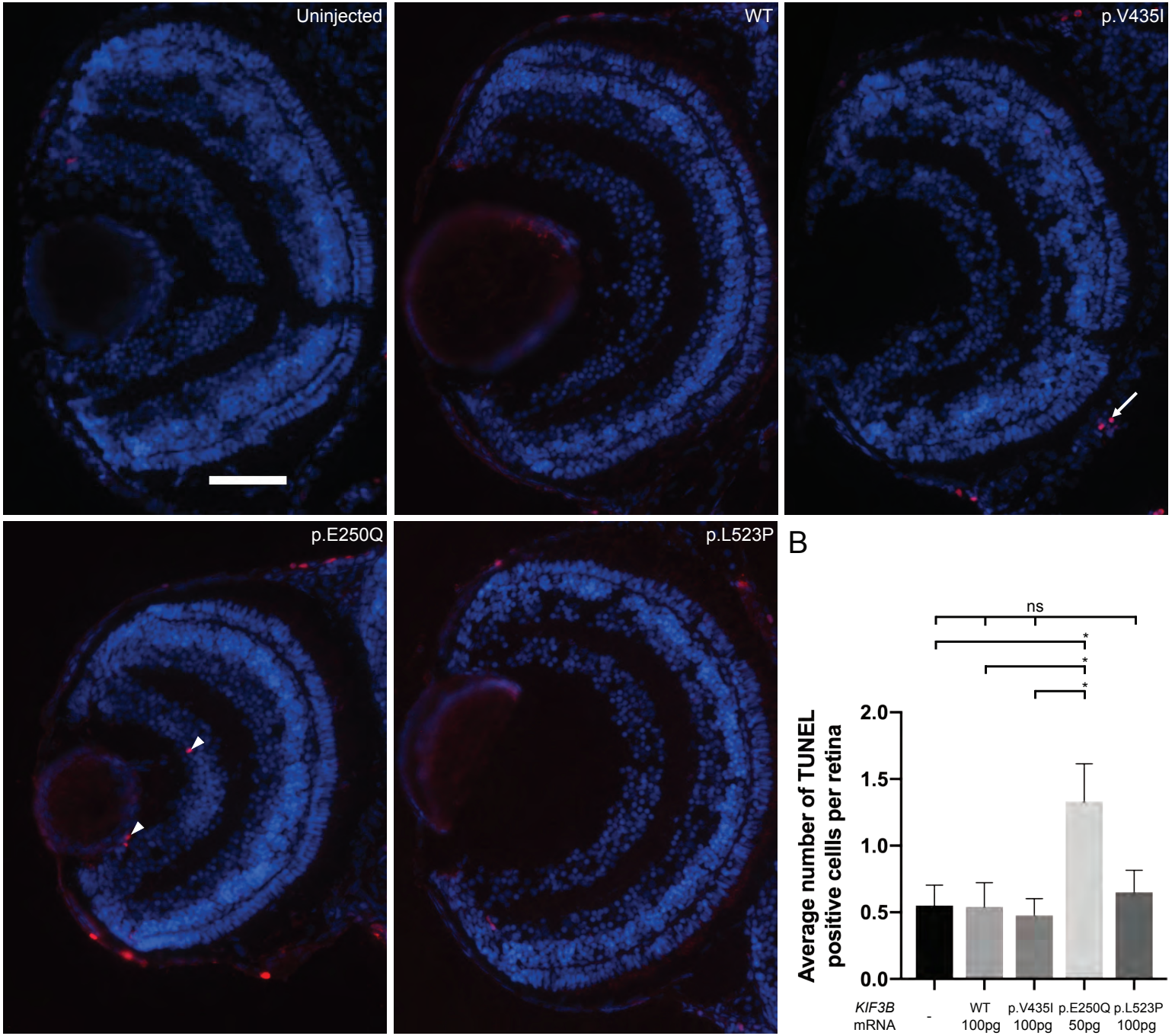
Uninjected
WT
p.V435I
p.E250Q
p.L523P
B
ns
*
*
*
Average number of TUNEL positive cells per retina
2.0
1.5
1.0
0.5
0.0
KIF3B mRNA
-
WT 100pg
p.V435I 100pg
p.E250Q 50pg
p.L523P 100pg

Figure S7

Figure S7. Zebrafish larvae injected with mRNA encoding p.Glu250Gln display increased cell death in the retina at 5 dpf.

(A) Representative images of optic sections obtained from 5 dpf larvae and stained with the Apotag Red In situ apoptosis detection kit (Millipore). White arrow heads indicate terminal deoxynucleotidyl transferase dUTP nick-end labeling (TUNEL) positive cells in the retina and the white arrow indicates a TUNEL positive cell outside of the retina (positive control). Scale bar: 50 μm, with equivalent scaling for each condition.

(B) Quantification of TUNEL positive cells at 5 dpf. n=10-13 larvae per condition, repeated twice with similar results. Error bars indicate standard error of the mean (s.e.m.).

Statistical comparison was performed with a non-parametric one-way ANOVA followed by Tukey's multiple comparison (GraphPad PRISM software; version 7.0c). * $p<0.05$. ns, not significant; WT, wild type; p.Glu250Gln and p.Leu523Pro are variants identified in cases; p.Val435Ile is a negative control (rs41288638; 230/276,748 alleles in gnomAD).

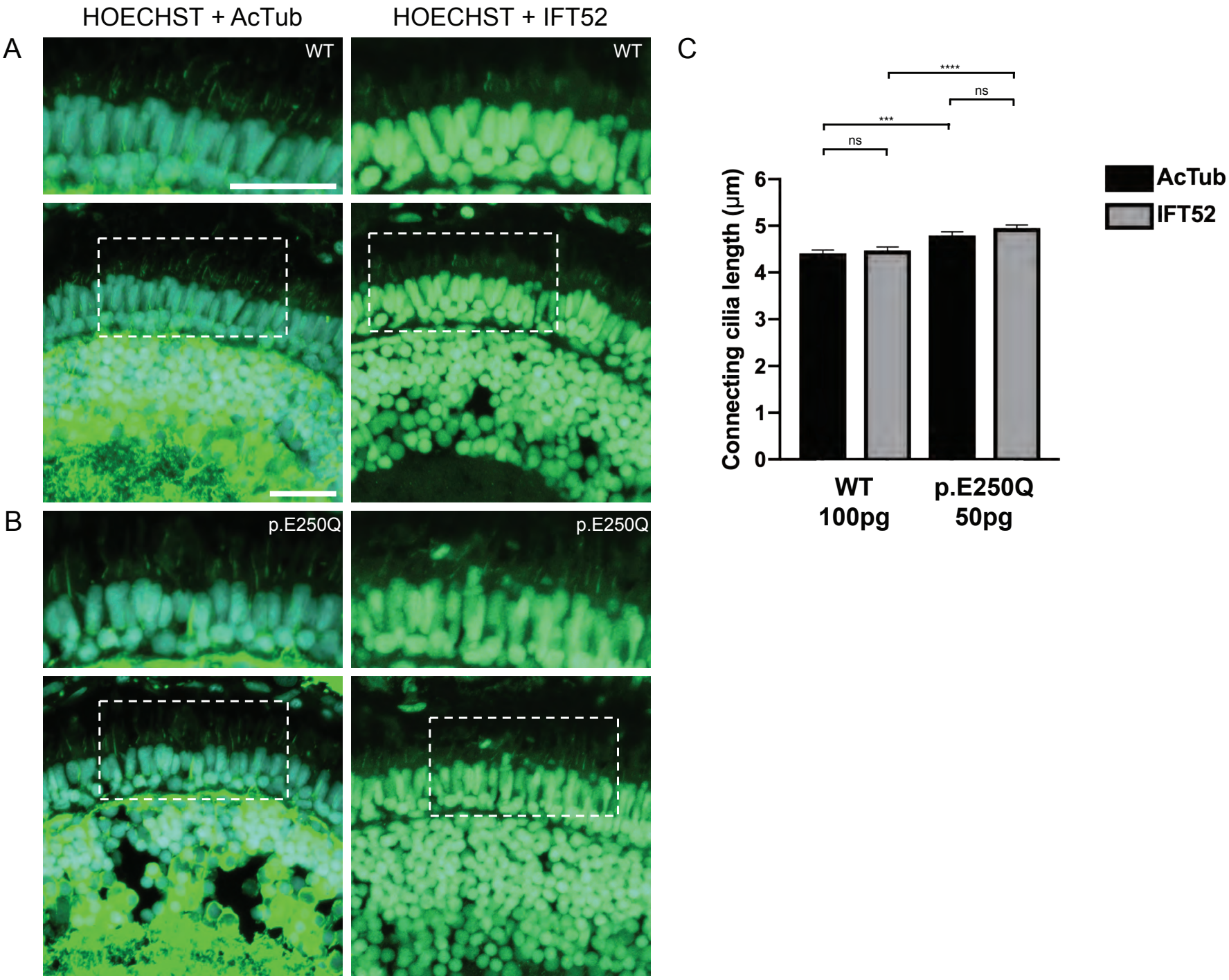
HOECHST + AcTub
HOECHST + IFT52
A
WT
WT
B
p.E250Q
p.E250Q
C
****
ns
***
ns
Connecting cilia length (µm)
0
1
2
3
4
5
6
AcTub
IFT52
WT
100pg
p.E250Q
50pg

Figure S8

Figure S8. Retinal cilia length assessed by either ciliary axoneme or anterograde IFT markers is indistinguishable.

(A) Representative merged images of optic sections obtained from 5 dpf larvae and stained with ciliary markers acetylated α-tubulin mouse monoclonal antibody (AcTub, ciliary axoneme) or anti-IFT52 rabbit polyclonal antibody (anterograde IFT) and Hoechst staining (nuclei); secondary detection was performed with the same fluorophore (Alexa Fluor 488) to test for altered anterograde IFT. Dashed white lines indicate the localization of the insets on top of each picture. Scale bars: 20 μm, with equivalent scaling for each condition.

(B) Quantification of photoreceptor connecting cilia length in 5 dpf zebrafish retinas. n=10-12 larvae per condition, n=97-246 cilia per retina, repeated twice with similar results. Error bars indicate standard error of the mean (s.e.m.). Statistical comparisons were performed with a non-parametric one-way ANOVA followed by Tukey's multiple comparison (GraphPad PRISM software; version 7.0c). ****$p<0.0001$; ns, not significant; WT, wild type; p.Glu250Gln was identified in the family A proband; See Table S3 for antibodies used.

Table S3. Antibodies used to study the effect of KIF3B dysfunction in cells, cat, and zebrafish.

Primary Antibody and Source	Application	Type	Primary Dilution	Secondary Antibody and Source	Secondary Dilution
Arl13b (ADP ribosylation factor like GTPase 13B) 17711-1-AP; Proteintech, Manchester, UK	Cilia marker in primary fibroblasts and hTERT-RPE1 cells	Polyclonal rabbit	1:500	Alexa Fluor 568 or 594 Goat anti-rabbit IgG Life Technologies, Carlsbad, CA, USA	1:1,000
γ-tubulin (gamma tubulin) T6557; Sigma-Aldrich, St. Quentin Fallavier Cedex, France	Centrosome marker in primary fibroblasts and hTERT-RPE1 cells	Monoclonal mouse	1:1,000	Alexa Fluor 488 Goat anti-mouse IgG Life Technologies, Carlsbad, CA, USA	1:1,000
c-myc 9E10; Santa Cruz Biotechnology, Santa Cruz, CA, USA,	IB of protein lysates from HEK293 cells	Monoclonal mouse	1:1,000	IRDyeVR 680RD Goat anti-mouse 925-68070; Li-Cor Biosciences, Lincoln, NE, USA	1:1,000
Actin A2066, Millipore Sigma, St. Louis, MO, USA	IB of protein lysates from HEK293 cells (loading control)	Polyclonal rabbit	1:1,000	IRDyeVR 800CW Goat anti-rabbit 925-32211; Li-Cor Biosciences, Lincoln, NE, USA	1:1,000
Kif3b (Kinesin like-protein 3B) 13817; Cell Signaling, Danvers, MA, USA	IHC in cat retina	Polyclonal rabbit	1:100	Alexa Fluor 488 Goat anti-rabbit IgG Life Technologies, Carlsbad, CA, USA	1:500
ML Opsin (Anti-Opsin, Red/Green; Medium/ Long wavelength cone opsin) AB5405; Millipore Corp., Billerica, MA, USA	IHC in cat retina	Polyclonal rabbit	1:1,000	Alexa Fluor 568 or 594 Goat anti-rabbit IgG Life Technologies, Carlsbad, CA, USA	1:500
PNA (Biotinylated Peanut Agglutinin) B-1075; Vector Labs Inc., Burlingame, CA, USA	IHC in cat retina	Biotinylated Lectin	1:500	Alexa Fluor 488 Streptavadin Life Technologies, Carlsbad, CA, USA	1:500
RetP1 (Rhodopsin Ab-1) MS-1233; Thermo Scientific, Rockford, IL, USA	IHC in cat retina	Monoclonal mouse	1:2	Alexa Fluor 594 Rabbit anti-mouse IgG Life Technologies, Carlsbad, CA, USA	1:500
Rhodopsin MABN15; Millipore Sigma, St. Louis, MO, USA	IHC in zebrafish retina	Monoclonal mouse	1:1,000	Alexa Fluor 488 Goat anti-mouse IgG Life technologies, Carlsbad, CA, USA	1:500
α-acetylated tubulin (alpha acetylated tubulin) T7451, Millipore Sigma, St. Louis, MO, USA	Cilia marker (IHC) in zebrafish retina	Monoclonal mouse	1:1,000	Alexa Fluor 647 Goat anti-rabbit IgG Life Technologies, Carlsbad, CA, USA	1:500
IFT52 (intraflagellar transport 52) gift from Brian Perkins	Anterograde IFT marker (IHC) in zebrafish retina	Polyclonal rabbit	1:5,000	Alexa Fluor 488 Goat anti-rabbit IgG Life Technologies, Carlsbad, CA, USA	1:500

IB, Immunoblotting; IFT, Intraflagellar transport; IHC, Immunohistochemistry

Table S4. Mutagenesis primers used to develop KIF3B mutant plasmids.

KIF3B_748 GC_FOR	cttggcttgccgttggctgccagcaagat
KIF3B_748 GC_REV	atcttgctggcagccaacggcaagccaag
KIF3B_1568 TC_FOR	gagctgtatgtctctttaggttccaaggtctcctcat
KIF3B_1568 TC_REV	atgaggagaccttggaacctaaagagacatacagctc
KIF3B_1303 GA_FOR	catcttctcctctgcaatcaagctgtgatcctcta
KIF3B_1303 GA_REV	tagaggatcacagcttgattgcagaggagaagatg

Table S5. SNPs associated with Bengal Progressive Retinal Atrophy (PRA) from GWAS. *SNP position is based on cat genome assembly FELIS_CATUS_9.0. SNP in bold is closest to *KIF3B*.

SNP Name	Chr	Position*	Association	Bonferroni	Fdr
chrA3.105500036	chrA3	83071208	2.34E-07	0.009966	0.009666
chrA3.104236810	chrA3	82014620	5.87E-07	0.024987	0.009666
chrA3.105245348	chrA3	82843004	6.82E-07	0.028999	0.009666
chrA3.104665241	chrA3	82352814	1.31E-06	0.055786	0.013939
chrUn13.2937466	chrF2	81618955	2.17E-06	0.092295	0.013939
chrA3.106515546	chrA3	83889737	2.23E-06	0.094678	0.013939
chrA3.1044673	**chrA3**	**27964631**	**2.29E-06**	**0.097572**	**0.013939**
chrA3.104098980	chrA3	81904276	6.12E-06	0.260376	0.02928
chrA3.103214225	chrA3	81167532	6.46E-06	0.274758	0.02928
chrA1.124658893	chrA1	1.07E+08	6.88E-06	0.2928	0.02928
chrA3.102843040	chrA3	80870525	1.08E-05	0.457434	0.035045
chrA3.102942692	chrA3	80945609	1.08E-05	0.457434	0.035045
chrA3.141313104	chrA3	1.31E+08	1.14E-05	0.485518	0.035045
chrA3.102918437	chrA3	80925955	1.15E-05	0.490625	0.035045
chrA3.106086700	chrA3	83554809	1.71E-05	0.726363	0.048424
chrA3.102884653	chrA3	80901583	1.95E-05	0.828487	0.049695
chrA3.105824159	chrA3	83341736	2.12E-05	0.902953	0.049695
chrE2.57091972	chrE2	47347454	2.12E-05	0.902953	0.049695
chrA3.101941266	chrA3	80124187	2.30E-05	0.977845	0.049695
chrA3.153780932	chrA3	1.4E+08	2.82E-05	1	0.049695
chrA3.15349133	chrA3	12823090	3.07E-05	1	0.049695
chrA3.147578832	chrA3	1.36E+08	3.07E-05	1	0.049695
chrA3.147780854	chrA3	1.36E+08	3.07E-05	1	0.049695
chrA3.148475337	chrA3	1.36E+08	3.07E-05	1	0.049695
chrA3.149716255	chrA3	1.37E+08	3.07E-05	1	0.049695
chrA3.150600799	chrA3	1.38E+08	3.07E-05	1	0.049695
chrA3.102772524	chrA3	80814167	3.16E-05	1	0.049695
chrUn.22624182	chrB2	51868898	3.27E-05	1	0.049695
chrUn3.2051358	chrA1	1.71E+08	3.63E-05	1	0.05081
chrUn3.2015995	chrA1	1.71E+08	3.63E-05	1	0.05081
chrA3.102974562	chrA3	80975434	3.82E-05	1	0.05081
chrA3.103173709	chrA3	81130065	3.82E-05	1	0.05081
chrA3.134386489	chrA3	1.07E+08	4.45E-05	1	0.054114
chrA3.143059974	chrA3	1.32E+08	4.45E-05	1	0.054114
chrA3.147529959	chrA3	1.35E+08	4.45E-05	1	0.054114

Table S6. Candidate high and moderate effect variants from WGS on cat chromosome A3 (human chromosome 20).

Chromosome Position*	Reference/ Alternative	Alleles	Het	Hom	Gene Name	Variant Effect	Transcript†	Amino Acid Effect
A3:18858513	G/A	388	8	2	CHD6	5_prime_UTR_variant	ENSFCAT00000050387:c.-179G>A	
A3:26784019	**C/T**	**390**	**9**	**2**	**KIF3B**	**Missense variant**	**ENSFCAT00000022266:c.1000G>A**	**p.Ala334Thr**
A3:22425011	G/A	390	8	3	SRC	3_prime_UTR_variant	ENSFCAT00000067246:c.*1679C>T	
A3:7014174	A/G	390	9	3	CBLN4	3_prime_UTR_variant	ENSFCAT00000007053:c.544+3527A>G	
A3:23937190	C/T	388	9	3	ERGIC3	Splice region variant	ENSFCAT00000038278:c.368-4G>A	
A3:23889605	G/A	386	9	3	SPAG4	Missense variant	ENSFCAT00000003230:c.259C>T	p.His87Tyr
A3:24057100	-/T	330	10	3	UQCC1	5 prime UTR variant	ENSFCAT00000049200:c.-389dupT	
A3:24003105	T/C	390	10	3	CEP250	Missense variant	ENSFCAT00000003224:c.2069A>G	p.Lys690Arg
A3:23989272	A/G	390	10	3	CEP250	Missense variant	ENSFCAT00000003224:c.3176T>C	p.Ile1059Thr
A3:23983575	G/A	388	10	3	CEP250	Missense variant	ENSFCAT00000003224:c.4178C>T	p.Ala1393Val
A3:23889718	G/A	388	10	3	SPAG4	Missense variant	ENSFCAT00000003230:c.146C>T	p.Pro49Leu
A3:22810151	T/C	388	10	3	SAMHD1	3_prime_UTR_variant	ENSFCAT00000012967:c.*416T>C	

*Positions based on cat reference FELIS_CATUS_9.0. Variant associated with Bengal PRA in bold. Two cats of 195 in the 99 Lives dataset were blind (Hom for homozygous). Eight cats were known obligate carriers and one pedigreed Bengal cat in the dataset was the unexpected carrier (Het for heterozygous). †Cat transcript annotation based on Ensembl 94.

Supplementary Methods

Human subjects and whole exome sequencing

Human subjects research was performed in accordance with the local ethics boards at the Nantes University Hospital (Nantes, France) and the University of Texas Health Science Center (Houston, TX, USA).

Family A. We performed whole exome sequencing of the proband with the Agilent SureSelect Clinical Research Exome kit according to manufacturer's instructions and generated 75-bp paired-end reads that were then aligned to human genome hg19 by bwa mem (v0.7.3). We analyzed data following GATK's best practices (v3.4).

Family B. Sample preparation, exome capture, Illumina sequence alignment and variant calling were performed as described.[10]

Plasmids and site directed mutagenesis

We obtained a WT human *KIF3B* open reading frame (ORF) construct (GenBank, NM_004798.4; GeneCopoeia; MO177) and subcloned it into two different Gateway destination vectors: pCS2+-C-myc or pCS2+ using LR clonase II mediated recombination according to manufacturer's instructions (Thermo Fisher). We performed site directed mutagenesis as described,[11] and plasmids were sequence confirmed to ensure ORF integrity.

Cilia length studies in human fibroblasts and hTERT-RPE cells

Cell culture and transient transfections. Fibroblasts were grown following standard procedures in AmnioMAX C-100 Complete Medium at 37°C and 5% CO_2 on labtek slides. hTERT-RPE1 cells were grown following standard procedures in DMEM-F12 Medium at 37°C and 5% CO_2 on labtek slides and transfected with jetPEI (Polyplus transfection®) at 70% confluency. Optimal serum deprivation (24 h) for primary cilium elongation in both cell types was performed.

Immunostaining. Human cultured fibroblasts and hTERT-RPE1 cells (48h post-transfection) were fixed at room temperature for 10 min in methanol (chilled at -20 °C), and then washed with PBS. Samples were permeabilized for 10 min with PBS containing 0.1% Triton-X100 (Sigma-Aldrich), then washed three times for 5 min. Samples were incubated with PBS containing 10% goat serum (Biowest) for 1h at room temperature. Primary antibodies were incubated at 4°C overnight. The primary antibodies mouse IgG1 anti-γ-tubulin (Sigma-Aldrich) and rabbit anti-Arl13b (Proteintech) were used to detect primary cilium morphology (basal body and axoneme, respectively; Table S3). Cells were washed with PBS, and then incubated with goat anti-mouse IgG1 coupled with AlexaFluor 488 (Life Technologies) and anti-rabbit

coupled with AlexaFluor 647 (Life Technologies) secondary antibodies for 2h at room temperature in the dark. Samples were washed and mounted with a solution of DAPI-Fluoromount-G® (SouthernBiotech; 00100-20) containing DAPI (4',6'-diamidino-2-phenylindole) for nuclear staining.

Image acquisition and analysis. 3D images of immunostained fibroblasts were captured using a Zeiss LSM700 confocal microscope equipped with a 63x 1.4 numerical aperture oil objective. To compare measured data, all confocal experiments showing ciliary length were acquired in the same conditions using slice thickness of 0.2 μm and a pixel size of 60 nm. Cilia length analysis was based on confocal Z-slices. The first method was used for primary and immortalized cultured cells to measure PC in 3D by Imaris v8.3 software (Bitplane). Serum deprivation allowed a maximal PC-stimulated elongation. This method allowed to normalized genotypes and offered precise value of PC lengths at a time given. In both cases, we double-checked PC length through staining with Arl13b and α-acetylated tubulin. Experiments with fibroblasts were replicated twice, and data were collected from six randomly selected fields imaged on each sample. Experiments with hTERT-RPE1 cells were performed on six independent experiments.

KIF3B Protein stability assays

Cell culture, transient transfections and cycloheximide treatment. HEK293 cells were grown following standard procedures in DMEM Medium at 37°C and 5% CO_2. We transfected cells with jetPEI (Polyplus transfection®) at 70% confluency, and then treated cells with 50 μm cycloheximide for 2h, and 4h post-transfection prior to protein harvest.

Immunoblotting. We prepared HEK293 cell lysates in RIPA buffer supplemented with protease-inhibitor cocktail tablets (cOmplete Mini, EDTA-free, 11836170001, Roche). Protein was migrated on a 4–12% NuPAGE polyacrylamide gel (Life Technologies, NP032B) at 140V for 100 min. The size-separated proteins were transferred to an Immobilon-FL membrane (Merck, IPFL00010) at 20V for 2 hours. After membrane blocking with Odyssey® Blocking Buffer (Li-Cor Biosciences, 927-40000), immunoblots were probed with mouse anti-c-myc and rabbit anti-actin antibodies (Table S3). Secondary detection was accomplished with goat anti-mouse and goat anti-rabbit antibodies using the Li-Cor system (Table S3). The obtained immunoreactivities were determined and calculated with ImageStudioLite software (Li-Cor Biosciences); three (cycloheximide studies) or six (untreated cells) biological replicates were performed for each experiment.

Cat phenotyping

Animals. All procedures were performed in accordance with the Association for Research in Vision and Ophthalmology (ARVO) statement for the Use of Animals in Ophthalmic and Vision Research and were approved by the relevant Institutional Animal Care and Use Committees.

Retinal morphology. Retinal immunohistochemistry (IHC) was performed on *Kif3b* mutant kittens at 8-, 20- and 34-weeks of age and wild type controls at 12-weeks of age. Frozen section immunohistochemistry of retinal cross sections was performed as described[12]. See Table S3 for antibodies used.

Cat genetic evaluations

Genome – wide association study (GWAS). Samples were ascertained as either whole EDTA blood from colony cats or buccal swabs donated by breeders and were prepared for GWAS as described.[1] DNAs from 44 cases and 54 controls were submitted to GeneSeek (Lincoln, NE) for genotyping on the Illumina Infinium iSelect 63K cat DNA array (Illumina, San Diego, CA).[2] GWAS for a case – control autosomal recessive trait was performed as described.[1] SNP genotyping rate and minor allele frequency (MAF) was calculated using PLINK[3]. SNPs with a MAF <5%, genotyping rate <90%, and individuals genotyped for <90% of SNPs were excluded from further analyses. A case-control association analysis was performed and corrected with 10,000 t-max permutations (-mperm 10,000). T-max permuted p-values were considered genome-wide significant at $p<0.05$. A Manhattan plot of the results was generated using HAPLOVIEW[4].

Whole genome sequencing (WGS). DNA for WGS was isolated by organic extraction from ~ 3 ml of EDTA anti-coagulated whole blood that was collected by jugular venipuncture. Approximately 4 µg of high molecular weight DNA from each cat was submitted to the University of Missouri DNA Core for sequencing library preparation and short-read sequencing as described[5]. The 350 bp and 550 bp libraries from all three cats were pooled and analyzed across nine lanes of a HiSeq 2000 (Illumina, Inc.).

Zebrafish phenotyping

Zebrafish husbandry and reagents for microinjection. All zebrafish studies were approved by the Duke University Institutional Animal Care and Use Committee. Zebrafish embryos were obtained by natural mating of wild-type (WT) hybrid TuAB[13] adults that were maintained on a 14h/10h light-dark cycle. Embryos were reared in embryo media (0.3 g/L NaCl, 75 mg/L $CaSO_4$, 37.5 mg/L $NaHC0_3$, 0.003% methylene blue) at 28°C until phenotypic endpoints. To generate variant human mRNA encoding variants identified in cases (p.Glu250Gln, p.Leu523Pro), and the negative control (p.Val435Ile) we performed *in*

vitro mRNA transcription with the SP6 mMessage mMachine kit (Thermo Fisher) as described (Table S4)[11].

Zebrafish microinjections and phenotyping. We injected embryos at the one-to-four cell stage with human *KIF3B* mRNA (10 pg, 25 pg, 50 pg, or 100 pg). For eye size assessment, we anesthetized larvae with tricaine at 3 days post-fertilization (dpf); imaged them live with the Vertebrate Automated Screening Technology (VAST) Bioimager (Union Biometrica); and measured eye area and body length automatically with FishInspector software[14]. Zebrafish phenotyping was performed with the investigator masked to injection condition, and experiments were repeated at least twice.

Histology of zebrafish retinal sections. We fixed 5 dpf larvae with 4% paraformaldehyde overnight, incubated in 30% sucrose for 24 h, embedded larvae in OCT to generate 7 μm transverse cryosections for the following studies. To evaluate apoptosis, we performed TUNEL detection *in situ* with the ApopTag Red In situ apoptosis detection kit (Millipore) according to manufacturer's instructions. Subsequent to image acquisition with a 90i epifluorescent microscope (Nikon), we counted terminal deoxynucleotidyl transferase dUTP nick-end labeling (TUNEL) positive cells with Image J (NIH). To evaluate photoreceptor integrity in the zebrafish retina, we assessed rhodopsin localization. We performed primary detection with anti-rhodopsin mouse monoclonal antibody (Table S3) essentially as described[15]. Subsequent to image acquisition with a 90i epifluorescent microscope (Nikon), we defined a region of interest corresponding to the rod inner segment (RIS) using Image J (NIH) and measured the mean signal intensity normalized to background (Figure 5B). To measure cilia length in the zebrafish retina, we stained cryosections with anti-acetylated α-tubulin mouse monoclonal antibody and anti-IFT52 rabbit polyclonal antibody (Table S3) as described[16]; nuclei were stained with Hoechst 33342. Z-stack images were acquired with the confocal module of the 90i microscope (90i) and merged in Image J (NIH) using the maximum intensity function. Connecting cilia were highlighted by both antibodies and measured using the segmented line tool.

Statistical comparisons.

Statistical comparisons were performed with two-tailed unpaired t-test (densitometry of immunoblotting) or a non-parametric one-way ANOVA followed by Tukey's multiple comparison (cilia length in cells; eye size, body length, cilia length or apoptosis in zebrafish) using GraphPad PRISM software. Significance was defined as $p<0.05$.

References

1. Ofri, R., Reilly, C.M., Maggs, D.J., Fitzgerald, P.G., Shilo-Benjamini, Y., Good, K.L., Grahn, R.A., Splawski, D.D., and Lyons, L.A. (2015). Characterization of an Early-Onset, Autosomal Recessive, Progressive Retinal Degeneration in Bengal Cats. Invest. Ophthalmol. Vis. Sci. *56*, 5299–5308.

2. Gandolfi, B., Grahn, R.A., Creighton, E.K., Williams, D.C., Dickinson, P.J., Sturges, B.K., Guo, L.T., Shelton, G.D., Leegwater, P.A.J., Longeri, M., et al. (2015). COLQ variant associated with Devon Rex and Sphynx feline hereditary myopathy. Anim. Genet. *46*, 711–715.

3. Oh, A., Pearce, J.W., Gandolfi, B., Creighton, E.K., Suedmeyer, W.K., Selig, M., Bosiack, A.P., Castaner, L.J., Whiting, R.E.H., Belknap, E.B., et al. (2017). Early-Onset Progressive Retinal Atrophy Associated with an IQCB1 Variant in African Black-Footed Cats (Felis nigripes). Sci. Rep. *7*, 43918.

4. Lyons, L.A., Creighton, E.K., Alhaddad, H., Beale, H.C., Grahn, R.A., Rah, H., Maggs, D.J., Helps, C.R., and Gandolfi, B. (2016). Whole genome sequencing in cats, identifies new models for blindness in AIPL1 and somite segmentation in HES7. BMC Genomics *17*, 265.

5. Aberdein, D., Munday, J.S., Gandolfi, B., Dittmer, K.E., Malik, R., Garrick, D.J., Lyons, L.A., and 99 Lives Consortium (2017). A FAS-ligand variant associated with autoimmune lymphoproliferative syndrome in cats. Mamm. Genome Off. J. Int. Mamm. Genome Soc. *28*, 47–55.

6. Lyons, L.A., Fox, D.B., Chesney, K.L., Britt, L.G., Buckley, R.M., Coates, J.R., Gandolfi, B., Grahn, R.A., Hamilton, M.J., Middleton, J.R., et al. (2019). Localization of a feline autosomal dominant dwarfism locus: a novel model of chondrodysplasia. BioRxiv 687210.

7. Cingolani, P., Platts, A., Wang, L.L., Coon, M., Nguyen, T., Wang, L., Land, S.J., Lu, X., and Ruden, D.M. (2012). A program for annotating and predicting the effects of single nucleotide polymorphisms, SnpEff: SNPs in the genome of Drosophila melanogaster strain w1118; iso-2; iso-3. Fly (Austin) *6*, 80–92.

8. Kumar, P., Henikoff, S., and Ng, P.C. (2009). Predicting the effects of coding non-synonymous variants on protein function using the SIFT algorithm. Nat. Protoc. *4*, 1073–1081.

9. Adzhubei, I.A., Schmidt, S., Peshkin, L., Ramensky, V.E., Gerasimova, A., Bork, P., Kondrashov, A.S., and Sunyaev, S.R. (2010). A method and server for predicting damaging missense mutations. Nat. Methods *7*, 248–249.

10. Koboldt, D.C., Larson, D.E., Sullivan, L.S., Bowne, S.J., Steinberg, K.M., Churchill, J.D., Buhr, A.C., Nutter, N., Pierce, E.A., Blanton, S.H., et al. (2014). Exome-based mapping and variant prioritization for inherited Mendelian disorders. Am. J. Hum. Genet. *94*, 373–384.

11. Niederriter, A.R., Davis, E.E., Golzio, C., Oh, E.C., Tsai, I.-C., and Katsanis, N. (2013). In vivo modeling of the morbid human genome using Danio rerio. J. Vis. Exp. JoVE e50338.

12. Mowat, F.M., Gornik, K.R., Dinculescu, A., Boye, S.L., Hauswirth, W.W., Petersen-Jones, S.M., and Bartoe, J.T. (2014). Tyrosine capsid-mutant AAV vectors for gene delivery to the canine retina from a subretinal or intravitreal approach. Gene Ther. *21*, 96–105.

13. Nasiadka, A., and Clark, M.D. (2012). Zebrafish breeding in the laboratory environment. ILAR J. *53*, 161–168.

14. Teixidó, E., Kießling, T.R., Krupp, E., Quevedo, C., Muriana, A., and Scholz, S. (2019). Automated Morphological Feature Assessment for Zebrafish Embryo Developmental Toxicity Screens. Toxicol. Sci. Off. J. Soc. Toxicol. *167*, 438–449.

15. Liu, Y.P., Bosch, D.G.M., Siemiatkowska, A.M., Rendtorff, N.D., Boonstra, F.N., Möller, C., Tranebjærg, L., Katsanis, N., and Cremers, F.P.M. (2017). Putative digenic inheritance of heterozygous RP1L1 and C2orf71 null mutations in syndromic retinal dystrophy. Ophthalmic Genet. *38*, 127–132.

16. Krock, B.L., and Perkins, B.D. (2008). The intraflagellar transport protein IFT57 is required for cilia maintenance and regulates IFT-particle-kinesin-II dissociation in vertebrate photoreceptors. J. Cell Sci. *121*, 1907–1915.